RACSAM (2012) 106:225–234
DOI 10.1007/s13398-011-0053-3

ORIGINAL PAPER

Discrete Lagrange-d'Alembert-Poincaré equations for Euler's disk

Cédric M. Campos · Hernán Cendra · Viviana Alejandra Díaz · David Martín de Diego

Received: 21 February 2011 / Accepted: 31 October 2011 / Published online: 18 November 2011

Abstract Nonholonomic systems are described by the Lagrange-d'Alembert principle. The presence of symmetry leads to a reduced d'Alembert principle and to the Lagrange-d'Alembert-Poincaré equations. First, we briefly recall from previous works how to obtain these reduced equations for the case of a thick disk rolling on a rough surface using a three-dimensional abelian group of symmetries. The main results of the present paper are the calculation of the discrete Lagrange-d'Alembert-Poincaré equations for an Euler's disk and the numerical simulation of a trajectory and its energy behavior.

Keywords Euler's disk · Discrete Lagrange-d'Alembert-Poincaré equations

Mathematics Subject Classification (2000) 53Z · 70F25 · 70H · 37J

1 Introduction

In the last years, an extraordinary effort has been given to the study of Lagrangian reduction and reconstruction for mechanical systems with Lie group symmetries. In the presence of constraints, it is necessary to modify the equations of motion to incorporate force

C. M. Campos · D. Martín de Diego
Instituto de Ciencias Matemáticas, Campus de Cantoblanco, UAM,
C/ Nicolás Cabrera, 15, 28049 Madrid, Spain
e-mail: cedricmc@icmat.es

D. Martín de Diego
e-mail: david.martin@icmat.es

H. Cendra · V. A. Díaz (✉)
Departamento de Matemática, Universidad Nacional del Sur,
Av. Alem 1253, 8000 Bahía Blanca, Argentina
e-mail: viviana.diaz@uns.edu.ar

H. Cendra
CONICET, Buenos Aires, Argentina
e-mail: hcendra@uns.edu.ar

constraints introduced using the classical Lagrange-d'Alembert's principle. This principle imposes restrictions on the set of infinitesimal variations (or constrained forces) in terms of the constraint functions (see [2,3,11]). The reduced equations are notably simplified in many interesting cases, thus facilitating the study of the dynamics, even allowing the integration of the equations of motion in some particular cases. However, this is not the general case, therefore it is necessary to use numerical methods to simulate the trajectories of the system. Recent works, such as [9,13], have introduced numerical integrators for nonholonomic systems with very good energy behavior and properties such as the preservation of the discrete nonholonomic momentum map (see also [15,16,18]).

Recently, there has been a renewed interest in the study of the dynamics of Euler's disk (see, for instance, [4,12,21]), specially motivated by Moffat's paper [23] (see also [1,5,14,19,24–27]). In this controversial paper, the ever-intriguing motions of a rolling disk is discussed. For nonholonomic systems with symmetries, e.g. Euler's disk, for the analysis of the equations of motion, it is interesting to use geometric reduction techniques. These methods were introduced in [6] and are based on the notion of nonholonomic connection. This connection is adapted to the nonholonomic distribution and to the symmetry of the problem simultaneously. It allows us to split the reduced equations in vertical and horizontal Lagrange-d'Alembert-Poincaré equations. Then, we summarize the derivation of the reduced equations for the case of a thick disk rolling on a rough surface (for details, see [7,8]). As a main result, we introduce a nonholonomic integrator for Euler's disk given by the discrete Lagrange-d'Alembert-Poincaré equations, and we exhibit its geometric preservation properties numerically. Our idea is to show that these new numerical methods are notably precise and can be used in more involved situations, for instance, when introducing some dissipative forces on the system simulating a more realistic case.

2 Reduced equations for Euler's disk

2.1 Lagrange-d'Alembert-Poincaré equations

Let $\pi : Q \to Q/G$ be a principal bundle with structure group G and we denote by $\mathscr{V}$ the vertical distribution. We assume that there is a given G-invariant (non-integrable) distribution $\mathscr{D}$ on Q. As in [6], we also assume that $TQ = \mathscr{D} + \mathscr{V}$. Let $\mathscr{S} = \mathscr{D} \cap \mathscr{V}$. Choosing a G-invariant metric on Q, we can define uniquely a principal connection form $\mathscr{A} : TQ \to \mathfrak{g}$ such that the associated horizontal distribution $\mathrm{Hor}^{\mathscr{A}} TQ$ satisfies the condition that, for each q, the space $\mathrm{Hor}^{\mathscr{A}} T_q Q$ coincides with the orthogonal complement of the space $\mathscr{S}_q$ in $\mathscr{D}_q$. This connection $\mathscr{A}$ is called a *nonholonomic connection* (see [6] for more details).

A given G-invariant Lagrangian $L : TQ \to \mathbb{R}$ naturally induces a reduced Lagrangian $\ell : TQ/G \to \mathbb{R}$. Since there exists a vector bundle isomorphism $\alpha_{\mathscr{A}} : TQ/G \to T(Q/G) \oplus \tilde{\mathfrak{g}}$, where $\tilde{\mathfrak{g}} = \mathrm{Ad}(Q)$ is the adjoint bundle of the principal bundle Q, we may think of ℓ as being a map $\ell : T(Q/G) \oplus \tilde{\mathfrak{g}} \to \mathbb{R}$ or, with the usual notation in terms of variables, $\ell(x, \dot{x}, \bar{v})$. Given any torsionless linear connection ∇ on Q/G we have a naturally defined connection $\nabla \oplus \tilde{\nabla}^{\mathscr{A}}$ on $T(Q/G) \oplus \tilde{\mathfrak{g}}$. In respect to this connection, the covariant derivatives $\dfrac{\partial^C \ell}{\partial x}$ and $\dfrac{D}{Dt}\dfrac{\partial \ell}{\partial \dot{x}}$ appearing in the following theorem should be understood (see [6] for details).

Theorem 1 (see [6]) *Let $q(t)$ be a curve in Q such that $(q(t), \dot{q}(t)) \in \mathscr{D}_{q(t)}$ and let $(x(t), \dot{x}(t), \bar{v}(t)) = \alpha_{\mathscr{A}}([q(t), \dot{q}(t)]_G)$ be the corresponding curve in $T(Q/G) \oplus \tilde{\mathfrak{s}}$, where $\tilde{\mathfrak{s}} = \alpha_{\mathscr{A}}(\mathscr{S}/G)$. The following conditions are equivalent.*

– *The **Lagrange-d'Alembert principle** holds:*

$$\delta \int_{t_0}^{t_1} L(q, \dot{q}) dt = 0 \,,$$

for any variation δq of the curve q such that $\delta q(t_i) = 0$, $i = 0, 1$, and $\delta q(t) \in \mathscr{D}_{q(t)}$.

– *The **vertical Lagrange-d'Alembert-Poincaré equation**, corresponding to vertical variations, holds:*

$$\frac{D}{Dt} \frac{\partial \ell}{\partial \bar{v}}(x, \dot{x}, \bar{v}) \bigg|_{\tilde{\mathfrak{s}}} = ad^*_{\bar{v}} \frac{\partial \ell}{\partial \bar{v}}(x, \dot{x}, \bar{v}) \bigg|_{\tilde{\mathfrak{s}}} \,;$$

*and as does hold the **horizontal Lagrange-d'Alembert-Poincaré equation**, corresponding to horizontal variations:*

$$\frac{\partial^C \ell}{\partial x}(x, \dot{x}, \bar{v}) - \frac{D}{Dt} \frac{\partial \ell}{\partial \dot{x}}(x, \dot{x}, \bar{v}) = \left\langle \frac{\partial \ell}{\partial \bar{v}}(x, \dot{x}, \bar{v}), \mathbf{i}_{\dot{x}} \tilde{B}(x) \right\rangle \,,$$

where $\tilde{B}$ is a $\tilde{\mathfrak{g}}$-valued 2-form on the base Q/G induced by $\mathscr{A}$ (see [6]).

2.2 Lagrange-d'Alembert-Poincaré equations for Euler's disk

Now, we shall recall from [8] the vertical and horizontal Lagrange-d'Alembert-Poincaré equations for Euler's disk. The reader may consult the above-mentioned paper for a more complete description of the system.

We consider Euler's disk as a thin cylinder, rolling without sliding on its rim on a horizontal rough plane. We assume that there is only one point of contact between the disk and the plane. The distribution of mass is assumed to have circular symmetry with respect to the axis perpendicular to the disk and passing through its geometric center, which coincides with the center of mass. So, two of the three principal moments of inertia are equal. Let us consider an Euler's disk of radius r and thickness re.

– The configuration space for Euler's disk is $Q =]0, \frac{\pi}{2}[\times S^1 \times S^1 \times \mathbb{R}^2$, and a point $q \in Q$ is written $q = (\theta, \varphi, \psi, x, y)$ as depicted in Fig. 1 (φ is the angle ϕ in the figure).
– The constraint distribution is given by

$$\mathscr{D}_{(\theta,\varphi,\psi,x,y)} = \left\{ (\theta, \varphi, \psi, x, y, \dot{\theta}, \dot{\varphi}, \dot{\psi}, \dot{x}, \dot{y}) \mid (\dot{x}, \dot{y}) = \dot{\psi} r u \right\} \,, \tag{1}$$

where u is the unitary vector $u = -(\cos\varphi, \sin\varphi)$ tangent to the disk at the contact point (x, y).

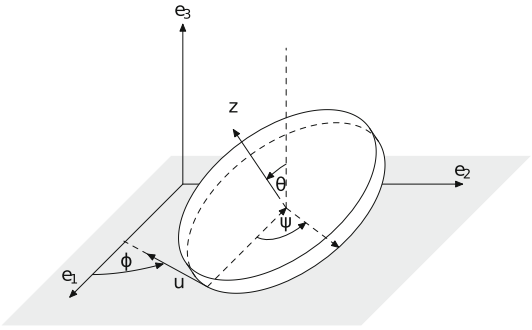

Fig. 1 Euler's disk

- The symmetry group $G = SO(2) \times \mathbb{R}^2$ acts on the right on Q by rotation and translation. Formally, the action of G is $R_{(\alpha,a,b)}(\theta, \varphi, \psi, x, y) = (\theta, \varphi, \psi + \alpha, x + a, y + b)$, for all $(\alpha, a, b) \in G$. This defines a principal fiber bundle $\pi : Q \to Q/G$.
- The vertical distribution $\mathscr{V}$ is given by

$$\mathscr{V}_{(\theta,\varphi,\psi,x,y)} = \left\{(\theta, \varphi, \psi, x, y, 0, 0, \dot{\psi}, \dot{x}, \dot{y})\right\} ,$$

  therefore the vector bundle $\mathscr{S} = \mathscr{D} \cap \mathscr{V}$ is

$$\mathscr{S}_{(\theta,\varphi,\psi,x,y)} = \left\{(\theta, \varphi, \psi, x, y, 0, 0, \dot{\psi}, \dot{x}, \dot{y}) \mid (\dot{x}, \dot{y}) = \dot{\psi} r u\right\}.$$

- We choose the horizontal distribution to be the vector bundle

$$\mathscr{H}_{(\theta,\varphi,\psi,x,y)} = \left\{(\theta, \varphi, \psi, x, y, \dot{\theta}, \dot{\varphi}, 0, 0, 0)\right\} ,$$

  which is associated to the connection 1-form $\mathscr{A} : TQ \to \widetilde{\mathfrak{g}} = \widetilde{\mathfrak{so}(2) \times \mathbb{R}^2}$ given by

$$\mathscr{A}(\theta, \varphi, \psi, x, y, \dot{\theta}, \dot{\varphi}, \dot{\psi}, \dot{x}, \dot{y}) = (\dot{\psi}, \dot{x}, \dot{y}).$$

- The subbundle $\tilde{\mathfrak{s}} \subset \widetilde{\mathfrak{g}}$ is then given by $\tilde{\mathfrak{s}} = \{(\dot{\psi}, \dot{\psi} r u)\}$.
- The $\tilde{\mathfrak{g}}$-valued 2-form $\tilde{B}$ is equal to zero because the horizontal distribution is integrable.
- We can write the Lagrangian $L : TQ \to \mathbb{R}$ of the system, given by the kinetic minus the potential energy, as follows

$$\begin{aligned}
&L(\theta, \varphi, \psi, x, y, \dot{\theta}, \dot{\varphi}, \dot{\psi}, \dot{x}, \dot{y}) \\
&\quad = \frac{1}{2} M r^2 \dot{\theta}^2 + \frac{1}{2} M r^2 \dot{\varphi}^2 \cos^2\theta + \frac{1}{2}\left(I_1 + \frac{1}{4} M r^2 e^2\right)(\dot{\theta}^2 + \dot{\varphi}^2 \sin^2\theta) \\
&\quad\quad + \frac{1}{2} I_3 (\dot{\varphi}\cos\theta + \dot{\psi})^2 + \frac{1}{2} M(\dot{x}^2 + \dot{y}^2) - \frac{1}{4} M r^2 e \dot{\varphi}^2 \sin 2\theta \\
&\quad\quad + M r \dot{x}\left(\dot{\theta}\sin\theta\sin\varphi - \dot{\varphi}\cos\theta\cos\varphi + \frac{1}{2} e(\dot{\varphi}\sin\theta\cos\varphi + \dot{\theta}\cos\theta\sin\varphi)\right) \\
&\quad\quad - M r \dot{y}\left(\dot{\theta}\sin\theta\cos\varphi + \dot{\varphi}\cos\theta\sin\varphi + \frac{1}{2} e(\dot{\varphi}\sin\theta\sin\varphi - \dot{\theta}\cos\theta\cos\varphi)\right) \\
&\quad\quad - g M r\left(\sin\theta + \frac{1}{2} e\cos\theta\right),
\end{aligned} \tag{2}$$

  where g is the acceleration of gravity, M is the mass of the disk, and $I_1 (= I_2)$, I_3 are the principal moments of inertia.
- From this Lagrangian, we obtain the reduced Lagrangian $\ell(\theta, \varphi, \dot{\theta}, \dot{\varphi}, \bar{v})$, where $\bar{v} = (\dot{\psi}, \dot{x}, \dot{y})$, which essentially has the same expression as L but different domain

$$\begin{aligned}
\ell(\theta, \varphi, \dot{\theta}, \dot{\varphi}, \bar{v}) &= \frac{1}{2} M r^2 \dot{\theta}^2 + \frac{1}{2} M r^2 \dot{\varphi}^2 \cos^2\theta + \frac{1}{2}\left(I_1 + \frac{1}{4} M r^2 e^2\right)(\dot{\theta}^2 + \dot{\varphi}^2 \sin^2\theta) \\
&\quad + \frac{1}{2} I_3 (\dot{\varphi}\cos\theta + \dot{\psi})^2 + \frac{1}{2} M(\dot{x}^2 + \dot{y}^2) - \frac{1}{4} M r^2 e \dot{\varphi}^2 \sin 2\theta \\
&\quad + M r \dot{x}\left(\dot{\theta}\sin\theta\sin\varphi - \dot{\varphi}\cos\theta\cos\varphi + \frac{1}{2} e(\dot{\varphi}\sin\theta\cos\varphi + \dot{\theta}\cos\theta\sin\varphi)\right) \\
&\quad - M r \dot{y}\left(\dot{\theta}\sin\theta\cos\varphi + \dot{\varphi}\cos\theta\sin\varphi + \frac{1}{2} e(\dot{\varphi}\sin\theta\sin\varphi - \dot{\theta}\cos\theta\cos\varphi)\right) \\
&\quad - g M r\left(\sin\theta + \frac{1}{2} e\cos\theta\right),
\end{aligned} \tag{3}$$

In order to simplify the forthcoming expressions, we redefine ℓ as $2\ell/Mr^2$ and we write $\bar{I}_i = I_i/Mr^2$ and $\bar{e} = e/2$. Then, the reduced Lagrangian takes the form

$$\begin{aligned}\ell(\theta,\varphi,\dot\theta,\dot\varphi,\bar v) = {}& \dot\theta^2 + \dot\varphi^2\cos^2\theta + \left(\bar I_1 + \bar e^2\right)\left(\dot\theta^2 + \dot\varphi^2\sin^2\theta\right)\\ &+ \bar I_3(\dot\varphi\cos\theta + \dot\psi)^2 + (\dot x^2 + \dot y^2)/r^2 - \bar e\dot\varphi^2\sin 2\theta\\ &+ 2\dot x\left(\dot\theta\sin\theta\sin\varphi - \dot\varphi\cos\theta\cos\varphi + \bar e(\dot\varphi\cos\varphi\sin\theta + \dot\theta\cos\theta\sin\varphi)\right)/r\\ &- 2\dot y\left(\dot\theta\sin\theta\cos\varphi + \dot\varphi\cos\theta\sin\varphi + \bar e(\dot\varphi\sin\varphi\sin\theta - \dot\theta\cos\theta\cos\varphi)\right)/r\\ &- 2g/r\,(\sin\theta + \bar e\cos\theta)\,.\end{aligned} \tag{4}$$

According to Theorem 1, we have the following system of Lagrange-d'Alembert-Poincaré equations for an Euler's disk (see [8] for details):

$$(\dot x, \dot y) = \dot\psi r u \tag{5}$$

$$\begin{aligned}0 = {}& \left((1+\bar I_3)\cos\theta - \bar e\sin\theta\right)\ddot\varphi + \bar I_3\ddot\psi + \langle(\ddot x,\ddot y), u\rangle/r\\ &- \left((2+\bar I_3)\sin\theta + 2\bar e\cos\theta\right)\dot\theta\dot\varphi\end{aligned} \tag{6}$$

$$\begin{aligned}0 = {}& \left((\bar I_1 + \bar e^2)\sin^2\theta + (1+\bar I_3)\cos^2\theta - \bar e\sin 2\theta\right)\ddot\varphi + \bar I_3\ddot\psi\cos\theta\\ &+ (\cos\theta - \bar e\sin\theta)\,\langle(\ddot x,\ddot y), u\rangle/r\\ &- \left((1 - \bar I_1 + \bar I_3 - \bar e^2)\sin 2\theta + 2\bar e\cos 2\theta\right)\dot\theta\dot\varphi - \bar I_3\dot\theta\dot\psi\sin\theta\end{aligned} \tag{7}$$

$$\begin{aligned}0 = {}& (1 + \bar I_1 + \bar e^2)\ddot\theta + \left((1 - \bar I_1 + \bar I_3 - \bar e^2)/2\sin 2\theta + \bar e\cos 2\theta\right)\dot\varphi^2\\ &+ \bar I_3\dot\varphi\dot\psi\sin\theta + (\sin\theta + \bar e\cos\theta)\,\langle(\ddot y, -\ddot x), u\rangle/r + g/r(\cos\theta - \bar e\sin\theta)\end{aligned} \tag{8}$$

By introducing the derivative of the rolling constraint (5) into the Eqs. (6–8), we obtain the following equivalent set of equations (recall that $u = -(\cos\varphi, \sin\varphi)$):

$$(\dot x, \dot y) = \dot\psi r u \tag{9}$$

$$\begin{aligned}0 = {}& \left((1+\bar I_3)\cos\theta - \bar e\sin\theta\right)\ddot\varphi + \bar I_3\ddot\psi + \langle(\ddot x,\ddot y), u\rangle/r\\ &- \left((2+\bar I_3)\sin\theta + 2\bar e\cos\theta\right)\dot\theta\dot\varphi\end{aligned} \tag{10}$$

$$\begin{aligned}0 = {}& \left((\bar I_1 + \bar e^2)\sin^2\theta + (1+\bar I_3)\cos^2\theta - \bar e\sin 2\theta\right)\ddot\varphi + \left((1+\bar I_3)\cos\theta - \bar e\sin\theta\right)\ddot\psi\\ &- \left((1 - \bar I_1 + \bar I_3 - \bar e^2)\sin 2\theta + 2\bar e\cos 2\theta\right)\dot\theta\dot\varphi - \bar I_3\dot\theta\dot\psi\sin\theta\end{aligned} \tag{11}$$

$$\begin{aligned}0 = {}& (1 + \bar I_1 + \bar e^2)\ddot\theta + \left((1 - \bar I_1 + \bar I_3 - \bar e^2)/2\sin 2\theta + \bar e\cos 2\theta\right)\dot\varphi^2\\ &+ \left((1+\bar I_3)\sin\theta + \bar e\cos\theta\right)\dot\varphi\dot\psi + g/r(\cos\theta - \bar e\sin\theta)\end{aligned} \tag{12}$$

3 Discrete equations for Euler's disk

In this section, we shall write a system of reduced discrete equations for the case of an Euler's disk and we shall numerically simulate it.

3.1 Discrete Lagrange-d'Alembert's principle

As it is well known, the dynamical equations of a Lagrangian system follow from a variational principle. Since the end of the last century, several researchers have been investigating numerical methods derived from an appropriate discretization of the variational principle (see [17,20]). From this discrete variational calculus, they derive the so-called discrete

Euler-Lagrange equations which produce a geometric integrator preserving symplecticity and momentun map.

For the case of Lagrangian systems with nonholonomic constraints, the problem is inherently more difficult since the nonholonomic flow is not preserving any symplectic form in general. Despite this problem, the construction of nonholonomic integrators was proposed in [10] (see also [9,22]), based on a discretization of the Lagrange-d'Alembert's principle. These methods do not preserve the symplectic form in the same way that the continuous nonholonomic flows does not preserve symplecticity, in general. They verify a discrete version of the nonholonomic momentum map and have an extraordinarily surprising energy behavior which remains bounded in all the worked examples, while the energy associated with a standard method decays due to numerical damping.

The idea of this section is to study the discretization and discrete reduction of Euler's disk with thickness. For this purpose, we will use the reduction methods developed by one of the authors and coworkers (see [18]) using the unifying approach of Lie groupoids.

We use the (local) discretization map $\tau_d\colon (Q\times Q)/G \to TQ/G$, where the configuration manifold is $Q = \left(0, \frac{\pi}{2}\right) \times S^1 \times S^1 \times \mathbb{R}^2$ and the symmetry group is $G = SO(2) \times \mathbb{R}^2$, given by

$$\tau_h(\theta_k, \theta_{k+1}, \varphi_k, \varphi_{k+1}, \kappa_k, \zeta_k, \eta_k) = \left(\theta_{k+\frac{1}{2}}, \varphi_{k+\frac{1}{2}}; \frac{\Delta\theta_k}{h}, \frac{\Delta\varphi_k}{h}, \frac{\kappa_k}{h}, \frac{\zeta_k}{h}, \frac{\eta_k}{h}\right)$$

where $\Delta\theta_k := \theta_{k+1} - \theta_k$, $\Delta\varphi_k := \varphi_{k+1} - \varphi_k$, $\theta_{k+\frac{1}{2}} := \frac{\theta_k+\theta_{k+1}}{2}$, $\varphi_{k+\frac{1}{2}} := \frac{\varphi_k+\varphi_{k+1}}{2}$ and $\kappa_k := \Delta\psi_k$, $\zeta_k := \Delta x_k$ and $\eta_k := \Delta y_k$.

Besides, observe that a section of the vector bundle $TQ/G \cong T\left[\left(0, \frac{\pi}{2}\right) \times S^1\right] \times \mathbb{R}^3$ is a pair (X, U) where X is a vector field on $\left(0, \frac{\pi}{2}\right) \times S^1$ and $U\colon \left(0, \frac{\pi}{2}\right) \times S^1 \to \mathbb{R}^3$ is a smooth map. Therefore, a basis of sections is

$$s_1 = \left(\frac{\partial}{\partial\theta}, 0\right), s_2 = \left(\frac{\partial}{\partial\varphi}, 0\right), s_3 = (0, E_1), s_4 = (0, E_2), s_5 = (0, E_3);$$

where $\{E_1, E_2, E_3\}$ is the canonical basis of $\mathbb{R}^3$.

We can determine a discrete nonholonomic system by the following three elements:

– The *reduced Lagrangian* is $\ell_d = h^2 \cdot (\ell \circ \tau_d)\colon (Q \times Q)/G \to \mathbb{R}$:

$$\begin{aligned}
&\ell_d(\theta_k, \theta_{k+1}, \varphi_k, \varphi_{k+1}, \kappa_k, \zeta_k, \eta_k)\\
&\quad = \Delta\theta_k^2 + \Delta\varphi_k^2 \cos^2\left(\theta_{k+\frac{1}{2}}\right) + \left(\bar{I}_1 + \bar{e}^2\right)\left(\Delta\theta_k^2 + \Delta\varphi_k^2 \sin^2\left(\theta_{k+\frac{1}{2}}\right)\right)\\
&\qquad + \bar{I}_3\left(\Delta\varphi_k \cos\left(\theta_{k+\frac{1}{2}}\right) + \kappa_k\right)^2 + \left(\zeta_k^2 + \eta_k^2\right)/r^2 - \bar{e}\Delta\varphi_k^2 \sin\left(2\theta_{k+\frac{1}{2}}\right)\\
&\qquad + 2\zeta_k\left(\Delta\theta_k \sin\left(\theta_{k+\frac{1}{2}}\right) \sin\left(\varphi_{k+\frac{1}{2}}\right) - \Delta\varphi_k \cos\left(\theta_{k+\frac{1}{2}}\right) \cos\left(\varphi_{k+\frac{1}{2}}\right)\right)/r\\
&\qquad + 2\zeta_k\bar{e}\left(\Delta\varphi_k \sin\left(\theta_{k+\frac{1}{2}}\right) \cos\left(\varphi_{k+\frac{1}{2}}\right) + \Delta\theta_k \cos\left(\theta_{k+\frac{1}{2}}\right) \sin\left(\varphi_{k+\frac{1}{2}}\right)\right)/r \quad (13)\\
&\qquad - 2\eta_k\left(\Delta\theta_k \sin\left(\theta_{k+\frac{1}{2}}\right) \cos\left(\varphi_{k+\frac{1}{2}}\right) + \Delta\varphi_k \cos\left(\theta_{k+\frac{1}{2}}\right) \sin\left(\varphi_{k+\frac{1}{2}}\right)\right)/r\\
&\qquad - 2\eta_k\bar{e}\left(\Delta\varphi_k \sin\left(\theta_{k+\frac{1}{2}}\right) \sin\left(\varphi_{k+\frac{1}{2}}\right) - \Delta\theta_k \cos\left(\theta_{k+\frac{1}{2}}\right) \cos\left(\varphi_{k+\frac{1}{2}}\right)\right)/r\\
&\qquad - 2h^2 g/r\left(\sin\left(\theta_{k+\frac{1}{2}}\right) + \bar{e}\cos\left(\theta_{k+\frac{1}{2}}\right)\right)
\end{aligned}$$

– The *discrete constraint submanifold* $\mathscr{M}_c$ of $(Q \times Q)/G$ is determined by the constraint functions

$$\zeta_k = -\kappa_k r \cos\varphi_{k+\frac{1}{2}} \quad \text{and} \quad \eta_k = -\kappa_k r \sin\varphi_{k+\frac{1}{2}}$$

– The *constraint distribution* $\mathscr{D}_c$ which is a vector subbundle of $TQ/G \to Q/G$ is given by

$$\mathscr{D}_c = \text{span}\,\{s_1, s_2, S_3 = s_3 - r\cos\varphi s_4 - r\sin\varphi s_5\}\,.$$

Observe that $\mathscr{D}_c = \mathscr{D}/G$ where $\mathscr{D}$ is defined in (1).

Following [18] the *discrete nonholonomic equations* are:

$$\begin{aligned}
\overleftarrow{s_1}\Big|_{(\theta_k,\theta_{k+1},\varphi_k,\varphi_{k+1},\kappa_k,\zeta_k,\eta_k)} l_d - \overrightarrow{s_1}\Big|_{(\theta_{k+1},\theta_{k+2},\varphi_{k+1},\varphi_{k+2},\kappa_{k+1},\zeta_{k+1},\eta_{k+1})} l_d = 0\\
\overleftarrow{s_2}\Big|_{(\theta_k,\theta_{k+1},\varphi_k,\varphi_{k+1},\kappa_k,\zeta_k,\eta_k)} l_d - \overrightarrow{s_2}\Big|_{(\theta_{k+1},\theta_{k+2},\varphi_{k+1},\varphi_{k+2},\kappa_{k+1},\zeta_{k+1},\eta_{k+1})} l_d = 0\\
\overleftarrow{S_3}\Big|_{(\theta_k,\theta_{k+1},\varphi_k,\varphi_{k+1},\kappa_k,\zeta_k,\eta_k)} l_d - \overrightarrow{S_3}\Big|_{(\theta_{k+1},\theta_{k+2},\varphi_{k+1},\varphi_{k+2},\kappa_{k+1},\zeta_{k+1},\eta_{k+1})} l_d = 0
\end{aligned}$$

$$\begin{aligned}
\zeta_k + \kappa_k r\cos\varphi_{k+\frac{1}{2}} = 0 \qquad & \eta_k + \kappa_k r\sin\varphi_{k+\frac{1}{2}} = 0\\
\zeta_{k+1} + \kappa_{k+1} r\cos\varphi_{k+1+\frac{1}{2}} = 0 \quad & \eta_{k+1} + \kappa_{k+1} r\sin\varphi_{k+1+\frac{1}{2}} = 0
\end{aligned}$$

where

$$\begin{aligned}
\overleftarrow{s_1} &= \frac{\partial}{\partial\theta_{k+1}}\,, \quad \overleftarrow{s_2} = \frac{\partial}{\partial\varphi_{k+1}}\,, \quad \overleftarrow{S_3} = \frac{\partial}{\partial\kappa_k} - r\cos\varphi_{k+1}\frac{\partial}{\partial\zeta_k} - r\sin\varphi_{k+1}\frac{\partial}{\partial\eta_k}\,,\\
\overrightarrow{s_1} &= -\frac{\partial}{\partial\theta_k}\,, \quad \overrightarrow{s_2} = -\frac{\partial}{\partial\varphi_k}\,, \quad \overrightarrow{S_3} = \frac{\partial}{\partial\kappa_k} - r\cos\varphi_k\frac{\partial}{\partial\zeta_k} - r\sin\varphi_k\frac{\partial}{\partial\eta_k}\,.
\end{aligned}$$

Substituting the constraints we derive the following system of equations which represents a geometric discretization of Eqs. (10–12):

$$\begin{aligned}
0 = {} & 4(1+\bar{I}_1+\bar{e}^2)(\Delta\theta_1 - \Delta\theta_0)\\
& + 2h^2 g/r(\cos(\theta_{0+\frac{1}{2}}) + \cos(\theta_{1+\frac{1}{2}}) - \bar{e}(\sin(\theta_{0+\frac{1}{2}}) + \sin(\theta_{1+\frac{1}{2}})))\\
& + \Delta\varphi_0^2((1-\bar{I}_1+\bar{I}_3-\bar{e}^2)\sin(2\theta_{0+\frac{1}{2}}) + 2\bar{e}\cos(2\theta_{0+\frac{1}{2}}))\\
& + \Delta\varphi_1^2((1-\bar{I}_1+\bar{I}_3-\bar{e}^2)\sin(2\theta_{1+\frac{1}{2}}) + 2\bar{e}\cos(2\theta_{1+\frac{1}{2}}))\\
& + 2\Delta\varphi_0\kappa_0((1+\bar{I}_3)\sin(\theta_{0+\frac{1}{2}}) + \bar{e}\cos(\theta_{0+\frac{1}{2}}))\\
& + 2\Delta\varphi_1\kappa_1((1+\bar{I}_3)\sin(\theta_{1+\frac{1}{2}}) + \bar{e}\cos(\theta_{1+\frac{1}{2}}))
\end{aligned} \tag{14}$$

$$\begin{aligned}
0 = {} & (1+\bar{I}_1+\bar{I}_3+\bar{e}^2)(\Delta\phi_1 - \Delta\phi_0)\\
& - \Delta\varphi_0((1-\bar{I}_1+\bar{I}_3-\bar{e}^2)\cos(2\theta_{0+\frac{1}{2}}) - 2\bar{e}\sin(2\theta_{0+\frac{1}{2}}))\\
& + \Delta\varphi_1((1-\bar{I}_1+\bar{I}_3-\bar{e}^2)\cos(2\theta_{1+\frac{1}{2}}) - 2\bar{e}\sin(2\theta_{1+\frac{1}{2}}))\\
& + \kappa_0((\Delta\theta_0+2n)\sin(\theta_{0+\frac{1}{2}}) - 2(1+\bar{I}_3-\bar{e}\Delta\theta_0/2)\cos(\theta_{0+\frac{1}{2}}))\\
& + \kappa_1((\Delta\theta_1-2n)\sin(\theta_{1+\frac{1}{2}}) + 2(1+\bar{I}_3+\bar{e}\Delta\theta_1/2)\cos(\theta_{1+\frac{1}{2}}))
\end{aligned} \tag{15}$$

$$0 = -\bar{I}_3(\Delta\phi_0\cos(\theta_{0+\frac{1}{2}}) - \Delta\phi_1\cos(\theta_{1+\frac{1}{2}}))$$

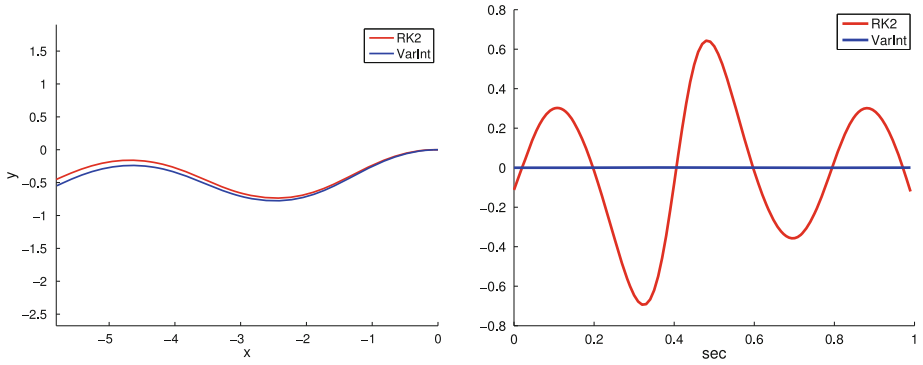

(a) Contact point's path **(b)** Energy function

Fig. 2 Step-size $h = 0.01$, iteration number $N = 100$

$$
\begin{aligned}
&-\kappa_0(\bar{I}_3 + \cos(\Delta\varphi_0/2)) \\
&+\kappa_1(\bar{I}_3 + \cos(\Delta\varphi_1/2)) \\
&-\Delta\varphi_0 \cos(\Delta\phi_0/2)(\cos(\theta_{0+\frac{1}{2}}) - \bar{e}\sin(\theta_{0+\frac{1}{2}})) \\
&+\Delta\varphi_1 \cos(\Delta\phi_1/2)(\cos(\theta_{1+\frac{1}{2}}) - \bar{e}\sin(\theta_{1+\frac{1}{2}})) \\
&-\Delta\theta_0 \sin(\Delta\phi_0/2)(\sin(\theta_{0+\frac{1}{2}}) + \bar{e}\cos(\theta_{0+\frac{1}{2}})) \\
&-\Delta\theta_1 \sin(\Delta\phi_1/2)(\sin(\theta_{1+\frac{1}{2}}) + \bar{e}\cos(\theta_{1+\frac{1}{2}}))
\end{aligned}
\tag{16}
$$

3.2 Numerical simulations of Euler's disk

The numerical simulations of Euler's disk have been carried out into Matlab using two different methods: the one proposed here; i.e., the variational integrator given by Eqs. (14–16); and a second order Runge–Kutta method applied to the continuous Eqs. (10–12). In order to represent a qualitative view of the solutions obtained by these methods, we have chosen to plot for each solution the path covered by the contact point of the disk and the total energy of the corresponding system, always comparing the variational integrator with the Runge–Kutta method.

The physical system is configured as follows: the gravity's acceleration is $g = 9.8$, the disk's mass $M = 1$, its radius $r = 1$, its thickness $re = 0.5$ and the principal moments of inertia are $I_1 = Mr^2/4 = 0.25$ and $I_3 = Mr^2/2 = 0.5$. The initial conditions are $q_0 = (\theta_0 = \pi/2, \varphi_0 = 0, \psi_0 = 0, x_0 = 0, y_0 = 0)$ and $q_1 = q_0 + h \cdot v_0$, where $v_0 = (\dot{\theta}_0 = \pi/8, \dot{\varphi}_0 = \pi, \dot{\psi}_0 = 2\pi, \dot{x}_1 = -2\pi r, \dot{y}_1 = 0)$ and h is the step size, which is $h = 0.01s$. For the simulation, we compute $N = 10.000$ iterations (points), of which Fig. 2a,b covers the first hundred (*i.e.* $T = 1s$), Fig. 3a,b covers the first thousand (*i.e.* $T = 10s$) and Fig. 4a,b covers the whole simulation (*i.e.* $T = 100s$).

The following aspects are worth noticing in the graphics: the contact point's path is "closed" for the variational integrator, while for the Runge–Kutta method slowly draws an inner spiral. The variational integrator maintains the geometric nature of the solution. Also, we may see that the energy for the variational integrator remains almost-constant, while for the Runge–Kutta method it oscillates within a bounded band having a small but non negligible decreasing slope.

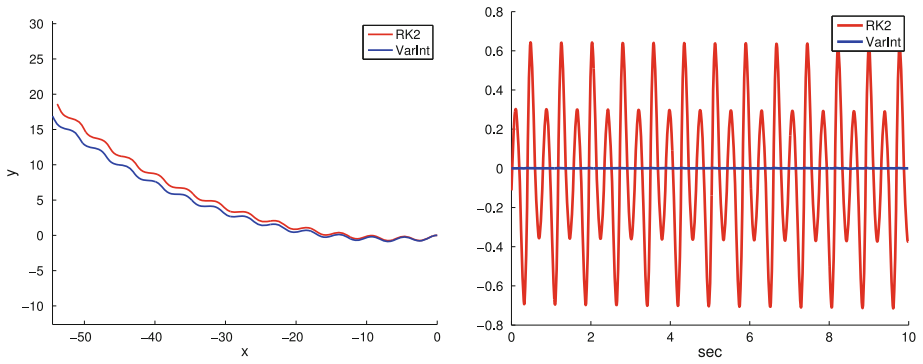

(a) Contact point's path **(b)** Energy function

Fig. 3 Step-size $h = 0.01$, iteration number $N = 1.000$

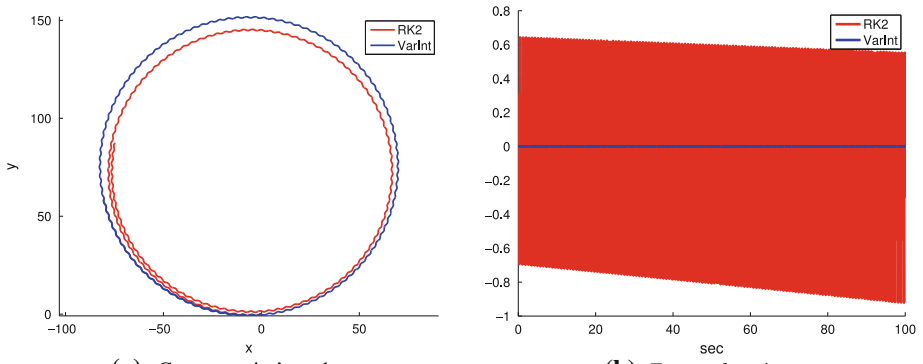

(a) Contact point's path **(b)** Energy function

Fig. 4 Step-size $h = 0.01$, iteration number $N = 10.000$

4 Conclusions and future work

In this paper, we first recall the Lagrange-d'Alembert-Poincaré equations for Euler's disk applying reduction by the symmetry group $SO(2) \times \mathbb{R}^2$. Then, using discrete variational calculus adapted to nonholonomic mechanics we derive a numerical method for Euler's disk. Finally, we implement some simulations showing its excellent energy behavior.

The knowledge of exact solutions and efficient numerical methods for Euler's disk should help to understand its behaviour under the addition of friction forces. One goal is to predict the finite-time singularity that appears when the disk falls flat (see [23] and subsequent discussion in [27]).

Acknowledgments We thank the referees for their helpful remarks. This work has been partially supported by MEC (Spain) MTM 2010-21186-C02-01, IRSES-project "Geomech-246981" and project "Geometric Mechanics and Control network" MTM 2009-08166-E. The authors C. M. Campos and V. Díaz acknowledge the MICINN and SGCyT, UNS, respectively, for former grants.

References

1. Bildsten, L.: Viscous dissipation for Euler disk. Phys. Rev. E. **66**, 056309 (2002)

2. Bloch, A.M.: Nonholonomic Mechanics and Control. Interdisciplinary Applied Mathematics Series, vol. 24. Springer, New-York (2003)
3. Bloch, A.M., Krishnaprasad, P.S., Marsden, J.E., Murray, R.M: Nonholonomic mechanical systems with symmetry. Arch. Ration. Mech. Anal. **136**, 21–99 (1996)
4. Borisov, A.V., Mamaev, I.S., Kilin, A.A.: Dynamics of rolling disk. Regul. Chaotic Dyn. **8**, 201–212 (2002)
5. Caps, H., Dorbolo, S., Ponte, S., Croisier, H., Vandewalle, N.: Rolling and slipping motion of Euler's disk. Phys. Rev. E **69**, 056610 (2004)
6. Cendra, H., Marsden, J.E., Ratiu, T.: Geometric Mechanics, Lagrangian reduction and Nonholonomic Systems. Mathematics Unlimited and Beyond. Springer, Berlin (2001)
7. Cendra, H., Díaz, V.A.: The Lagrange-d'Alembert-Poincaré equations and Integrability for the rolling disk. Regul. Chaotic Dyn. **11**(1), 67–81 (2006)
8. Cendra, H., Díaz, V.A: The Lagrange-d'Alembert-Poincaré equations and Integrability for the Euler's Disk. Regul. Chaotic Dyn. **12**(1), 56–67 (2007)
9. Cortés, J.: Geometric, control and numerical aspects of nonholonomic systems. Lecture Notes in Mathematics, vol. 1793. Springer, Berlin (2002)
10. Cortés, J., Martínez, S.: Nonholonomic integrators. Nonlinearity **14**(5), 1365–1392 (2001)
11. Cushman, R., Duistermaat, H., Sniatycki, J.: Geometry of nonholonomically constrained systems. Adv. Ser. Nonlinear Dyn. **26**, (2010)
12. Cushman, R., Hermans, J., Kemppainen, D.: The rolling disk. Nonlinear Differ. Equ. Appl. **19**, (1996)
13. de León, M., Martínde Diego, D., Santamaría-Merino, A.: Geometric integrators and nonholonomic mechanics. J. Math. Phys. **45**(3), 1042–1064 (2004)
14. Easwar, K., Rouyer, F., Menon, N.: Speeding to a stop: the finite-time singularity of a spinning disk. Phys. Rev. E **66**, 045102(R) (2002)
15. Fedorov, Y.N., Zenkov, D.V.: Discrete nonholonomic LL systems on Lie groups. Nonlinearity **18**, 2211–2241 (2005)
16. Fedorov, Y.N. and Zenkov, D.V.: Dynamics of the discrete Chaplygin sleigh. Discret. Contin. Dyn. Syst., 258–267 (2005)
17. Hairer, E., Lubich, C., Wanner, G.: Geometric Numerical Integration, Structure-Preserving Algorithms for Ordinary Differential Equations. Springer Series in Computational Mathematics, vol. 31. Springer, Berlin (2002)
18. Iglesias, D., Marrero, J.C., Martínde Diego, D., Martínez, E.: Discrete nonholonomic Lagrangian systems on Lie groupoids. J. Nonlinear Sci. **18**, 221–276 (2008)
19. Kessler, P., O'Reilly, O.M.: The ringing of Euler's disk. Regul. Chaotic Dyn. **7**, 49–60 (2002)
20. Marsden, J.E., West, M.: Discrete Mechanics and variational integrators. Acta Numer. **10**, 357–514 (2001)
21. McDonald, A.J., McDonald, K.T.: The rolling motion of a disk on a horizontal plane. e-print available at http://www.puhep1.princeton.edu/mcdonald/examples/rollingdisk.pdf and at http://www.lanl.gov/abs/physics/0008227 (2001)
22. McLachlan, R., Perlmutter, M.: Integrators for nonholonomic mechanical systems. J. Nonlinear Sci. **16**, 283–328 (2006)
23. Moffatt, H.K.: Euler's disk and its finite-time singularity. Nature **404**, 833–834 (2000)
24. Moffat, H.K.: Reply to G. van den Engh et al. Nature **408**, 540 (2000)
25. Petrie, D., Hunt, J.L., Gray, C.G.: Does the Euler disk slip during its motion?. Am. J. Phys. **70**, 1025 (2002)
26. Stanislavsky, A.A., Weron, K.: Nonlinear oscillations in the rolling motion of Euler's disk. Phys. D **156**, 247–259 (2001)
27. van den Engh, G., Nelson, P., Roach, J.: Numismatic gyrations. Nature **408**, 540 (2000)